Optics Letters

Thin-film dynamics unveils interplay between light momentum and fluid mechanics

Gopal Verma,[1,3] Gyanendra Yadav,[2] and Wei Li[1,*]

[1]GPL Photonics Lab, State Key Laboratory of Applied Optics, Changchun Institute of Optics, Fine Mechanics and Physics, Chinese Academy of Sciences, Changchun 130033, China
[2]School of Physical Sciences, University of Liverpool, Liverpool L69 3BX, UK
[3]e-mail: gopal@ciomp.ac.cn
*Corresponding author: weili1@ciomp.ac.cn

Received 3 November 2022; accepted 22 November 2022; posted 23 November 2022; published 21 December 2022

We quantitatively measure the nanomechanical dynamics of a water surface excited by the radiation pressure of a Gaussian/annular laser beam of incidence near total internal reflection (TIR). Notably, the radiation pressure near TIR allowed us to induce a pushing force (Abraham's momentum of light) for a wide annular Gaussian beam excitation of the thin-film regime of water, which, to the best of our knowledge, has never been observed with nanometric precision previously. Our finding suggests that the observation of either/both Abraham's and Minkowski's theories can be witnessed by the interplay between optics and fluid mechanics. Furthermore, we demonstrate the first, to the best of our knowledge, simultaneous measurement of Abraham's and Minkowski's momenta emerging in a single setup with a single laser shot. Our experimental results are strongly backed by numerical simulations performed with realistic experimental parameters and offer a broad range of light applications in optofluidics and light-actuated micromechanics.

https://doi.org/10.1364/OL.479860

The correct form of the momentum of light within a dielectric medium and the effects caused by radiation forces when light passes through adjacent media have been extensively debated for over a century [1–14]. The formulation of two different yet fundamental momenta [1,2], laid by Abraham and Minkowski for light in a refractive medium, has been recently identified as kinetic and canonical momenta, respectively [4–15]. Minkowski's theory has good experimental credentials because all the experimental results related to radiation pressure have demonstrated it with nanometer precision [16–18], backed with numerical simulations. Surprisingly, the first Abraham pressure of light [producing dimples at an air–water (AW) interface] was claimed [19,20] using an unfocused laser beam. But, the subsequent experiments could not reproduce the results [17,21] even with a technique of nanometric sensitivity. These conflicting experimental observations of fundamental momenta pose a bottleneck for the investigation of the true nature of light's momentum inside fluids and forces us to find the precise and correct parameters or configuration where the Abraham nature of momentum may appear.

As described in Refs. [18,22], pressure imparted by light to a liquid surface pushes the AW interface inward (Abraham pressure). However, the hydrostatic pressure counterbalances it due to electrostriction, and the resulting deformation is outward (forming a bulge on the AW interface) to the surface (Minkowski's momentum). Considering the dynamics of the experimental situation [3,18,23], it can be shown that the mechanical pressure in the liquid reaches equilibrium ($\tau = w/v_s$, where w is the pump beam waist and v_s is the sound velocity) which causes an outward bulge at the surface. However, thin-film dynamics behave differently from deep-water dynamics due to high viscous stresses, low impact of inertial forces, low velocity, and influence of surface tension, effective mostly at small scales (shallower water) [24]. This could provide a pertinent testbed for investigating the Abraham pressure of light.

In this Letter, we utilized a pump–probe-based setup to investigate the interplay between light momentum, which is greatly needed, given the historical difficulty in understanding light momentum. We used a time-resolved interferometric technique with <5 nm precision [16,25,26] to measure the nanoscale interface dynamics in thick/thin water films with Gaussian beam (GB) and annular GB excitation. Surprisingly, we observed that for the AW interface deformation in the thin-film regime ($d/w \ll 1$, where d is the thickness of water) in the case of wide annular GB excitation near total internal reflection (TIR), the pressure initially pushes the AW interface inward and then outward. This clearly indicates push (Abraham pressure) and pull (Minkowski pressure) forces in the same setup, that has never been studied with nanometric precision before. Finally, we present a simple yet sensitive method to quantitatively analyze nanoscale phenomena in liquids which govern the interplay between the nature of light momentum and fluid, paving the way for optofluidic applications [27,28].

A schematic of our setup is shown in Fig. 1. We placed a large water drop on a prism. The natural evaporation of water reduced the droplet thickness continuously. This resulted in dynamic interference fringes in probe beam and provided an oscillatory curve of intensity [$I_p(t)$, red curve in Fig. 2] when the central fringe was tracked [16,17]. We also controlled the evaporation rate ($\delta d/\delta t$) by partial enclosure to achieve stable, steady-state evaporation. The analysis of the interference fringe pattern with the baseline of the natural evaporation of

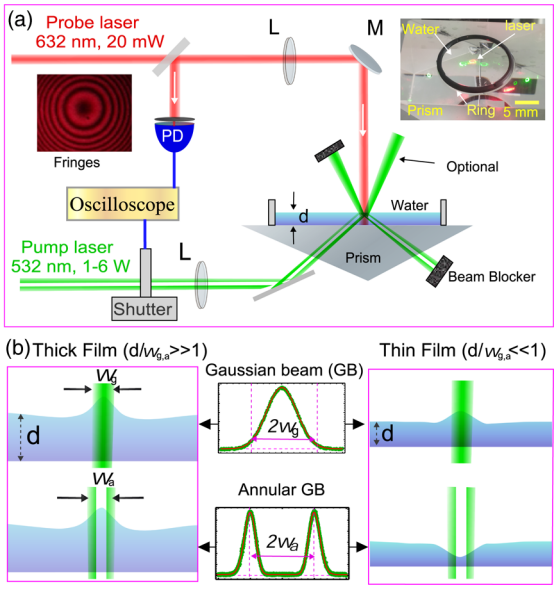

Fig. 1. (a) Schematic of experimental setup. A collimated He–Ne laser (λ = 632 nm, 10 mW, θ_i<5°) produces a dynamic interference pattern from an evaporating water drop. A green pump beam (λ = 532 nm, P = 1–5 W) is used to locally deform the water whose exposure time is controlled by an optical shutter. PD, photodiode; M, mirror. (b) Schematic for thick- and thin-film deformation under Gaussian and annular beams. Here T = 25 ± 1°C, 50% RH.

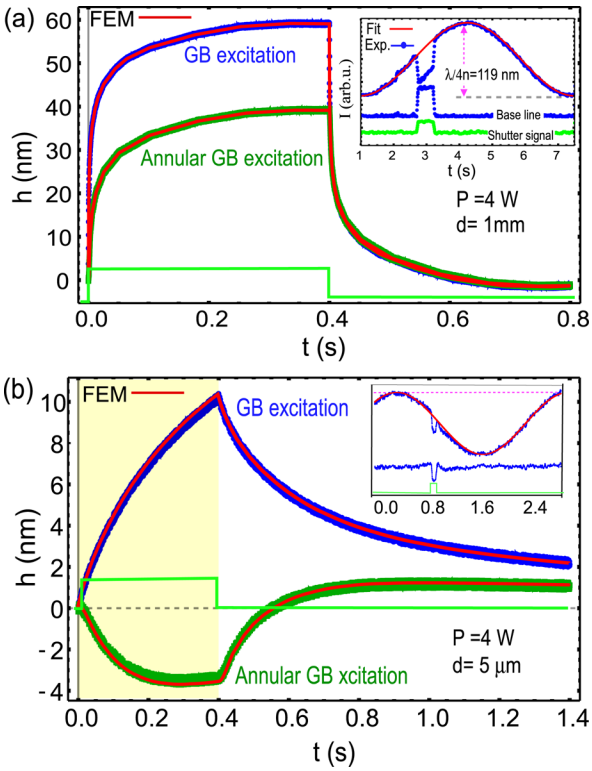

Fig. 2. (a) Time-resolved AW interface deformation (thick sample) height under GB (w_g = 250 μm) and annular GB (w_a = 500 μm) excitation. Inset: probe intensity $I(t)$ in terms of nanometers versus time for pump on–off cycles. The solid red line is a fit of $I_p(t)\cos^2(\alpha_0 d(t))$ to the simulated data (blue) corresponding to natural evaporation and pump beam excitation. (b) Time-resolved AW interface deformation (thin sample) height under GB and annular GB excitation.

water gave us the directional surface height variation with nanometer sensitivity (δd) subjected to optical force [16,17,24]. The key feature of using this technique is that it can cleanly measure the direction and magnitude of the nanometric surface deformation.

Firstly, we performed a requisite test with thick-water-film deformation induced by GB. For this, we directed a pump laser (w = 250 μm) incident near TIR at the AW interface. Light pressure induced a nanometric bulge on the AW interface, as shown in Fig. 2(a). We observed a nanoscale bump in both GB and annular GB excitation for a thick water sample. However, the bump magnitude is smaller for the annular GB due to the smaller light intensity. Zoom of the opening/closing duration of the shutter [Fig. 2(a)] showed that the AW interface adiabatically followed the pump beam as shown approximately by the exact rise/fall times for the green curves. This unambiguously demonstrated that the pump beam induced an increase in the height of the AW interface resulting in an outward bulge and supported Minkowski's form of momentum [17,18,24].

Notably, in the thin-film-regime case, we observed dimples during annular beam excitation, as shown in Fig. 2(b). However, the GB induced a bulge as for the thick film but on a different time scale as interface dynamics of thin film is governed by time scale ($\tau_{th} = 3\eta w_g^4/\gamma d^3$, where w_g is the Gaussian laser beam waist, η the viscosity, and γ the surface tension of the water) [24]. One could expect that light pressure does not have sufficient time to equilibrate the pressure across the laser spot. For this, we consider Ashkin and Dziedzic's experiments [3] concerning the forces on AW interfaces and the time scale of pressure equilibrium. They used high-intensity pulses (1 kW) of about 50 ns duration, focused to a small spot only a few wavelengths in diameter. With a spot radius of about 10 μm, and sound velocity of about 10^3 m/s, one may estimate that the mechanical pressure in the liquid does have enough time to approach equilibrium during the 50 ns pulse. Thus an outward force is expected, which results in an outward bulge on the surface where the beam passes. Figure 3(a) shows that beam waist dependence dynamics of the interface clearly demonstrates the inward pressure of light present during the laser exposure. One can see that for larger radii, dimples survive for a longer time. This is because of the large time scale involved [24] in the thin-film regime. Dimple is universally present at the center of the deformed surface, followed by a global bulge. The 1D height profiles of the AW interface at two different times are shown in Fig. 3(b).

In order to validate our experimental data, we compared them with numerical results. For a dielectric fluid in the absence of free charge and current, the momentum density is $\mathbf{G} = \mathbf{E} \times \mathbf{H}/c^2$ and force density is given by [18,22]

$$\mathbf{f} = -\frac{1}{2}\varepsilon_0\langle E\rangle^2\nabla\varepsilon_r + \frac{1}{2}\varepsilon_0\nabla\left[\rho\left(\frac{\partial\varepsilon_r}{\partial\rho}\right)_T\langle E\rangle^2\right] + (\varepsilon_r - 1)\frac{\partial\mathbf{G}}{\partial t}, \quad (1)$$

where ρ is the mass density, c is the speed of light, and $\varepsilon_r = \varepsilon/\varepsilon_0$ and $\mu_r = \mu/\mu_0$ are the relative permittivity and permeability of the medium, respectively. The first term in Eq. (1) is a common term arising from the Minkowski and Abraham energy momentum tensors. The second term is the electrostriction force and it is important when the field and dielectric permittivity are

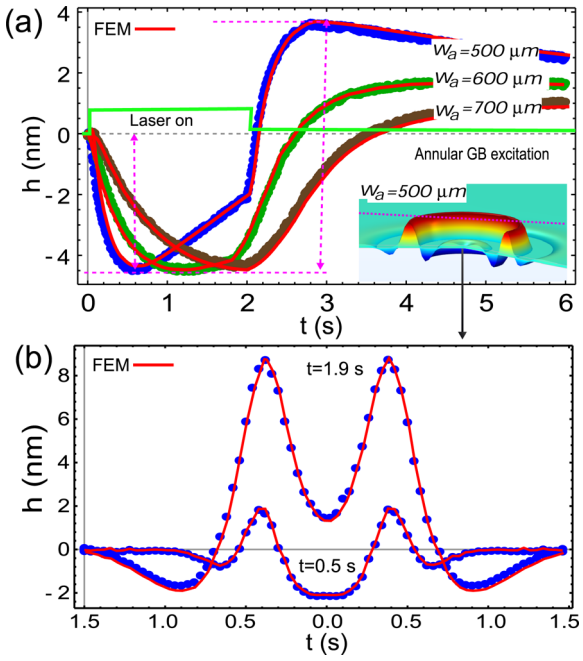

Fig. 3. (a) Time-resolved AW interface deformation (thick sample) height under GB and annular GB excitation. Inset: FEM simulated image of deformed AW interface. (b) 1D height profiles along the interface.

inhomogeneous. The last term is known as the Abraham force density and this term averages to zero at optical frequencies, hence Eq. (1) reduces to the Helmholtz force [18]. The pressure P imparted by the surface force can be calculated by integrating the normal component of $\mathbf{f}$ across the air–liquid interface as

$$P_{\text{in}} = \frac{1}{2}\varepsilon_0 \langle E_{\parallel} \rangle^2 \rho \left(\frac{\partial \varepsilon_r}{\partial \rho}\right)_T - \frac{1}{2}\varepsilon_0 \langle E_{\parallel} \rangle^2 (\varepsilon_r - 1). \quad \textbf{(2)}$$

The first term in Eq. (2) is the surface contribution of the electrostriction force and the second term is numerically the radiation pressure defined in the Minkowski momentum transfer formulation. The radial volume electrostriction force results in a pressure P_{in} pushing the surface inwards, which is compatible with the Abraham momentum. This pressure is counterbalanced by the hydrostatic pressure P_{out} due to electrostriction [18,22], which can be written with the help of Eq. (1) as

$$P_{\text{out}} = \frac{1}{2}\varepsilon_0 \rho \left(\frac{\partial \varepsilon_r}{\partial \rho}\right)_T \langle E_{\parallel} \rangle^2. \quad \textbf{(3)}$$

Using the relation $I(r,t) = \varepsilon_0 cn \langle E_{\text{inc}} \rangle^2$, the overall pressure that elevates the surface of the liquid is [18]

$$P(r,t) = P_{\text{in}} - P_{\text{out}} = -\frac{2}{c}\left(\frac{n-1}{n+1}\right) I(r,t). \quad \textbf{(4)}$$

This pressure is outward and induces a bulge on the AW interface, and equivalent to Minkowski's momentum or canonical momentum as the total propagating momentum. Many authors have verified this [3,16–18,21,22,24,29,30] experimentally/numerically under GB excitation for thick liquid film [3,16–18] for normal and general angle of incidence as well as pulsed and continuous lasers. In Ref. [24], the thin-film dynamics was also investigated, which allowed us to precisely measure an about 1 nm deformation height $h(t)$, because noise becomes very small in a thin film where viscous force dominates. Analytical solution of thin-film dynamics is complicated and still missing especially for annular-shape intensity profile. Therefore, we calculated it by solving the Navier–Stokes equation using the finite element method (FEM)-based software Comsol Multiphysics. The FEM has been used to predict how a system behaves in a great variety of conditions [18,21]. One can model an annular GB laser intensity profile to investigate the effect of the transient deformation profile of the AW interface. The effects of the radiation pressure on the surface displacement were calculated by solving the Navier–Stokes equation with appropriate boundary conditions. The Laminar Two-Phase Flow, Moving Mesh module was used to solve the Navier–Stokes equation for incompressible flow:

$$\rho \frac{dv}{dt} + \rho(v.\nabla)v = -\nabla P + \eta \nabla^2 v + F, \quad \textbf{(5)}$$

where v describes the flow velocity, P is the pressure, ρ is the fluid density, and η is the dynamic viscosity. The model was built in two-dimensional (2D) axisymmetric geometry.

The external pressure P and surface tension were made to act on the AW interface. For general angle of incidence, $P(\theta_i, r) = f(\theta_i) 2n(n-1) I(r)/c(n+1)$, where $f(\theta_i) = \cos^2\theta_i (1 + R - (\tan\theta_i/\tan\theta_t)T)$, $I(r)$ is the intensity of incident light beam, and θ_i and θ_t denote angles of incidence and transmission, respectively [16]. Free surface and no-slip boundary conditions were applied at the liquid and substrate interfaces $v_x(z=0) = 0$. The gravity vector entered the force term as $F = \rho g$ with $g = 9.8$ m/s^2 [18,21]. Realistic sample geometry was considered (Fig. 1; $R = 20$ mm and $h_0 = 0.01$–1 mm).

Annular shape of laser beam intensity distribution enters through the pressure term and can be modeled by

$$I(r) = P_0 \frac{2^{l+1} r^{2l}}{\pi l! w_g^{2(l+1)}} \exp\left[-2r^2/w_g^2\right].$$

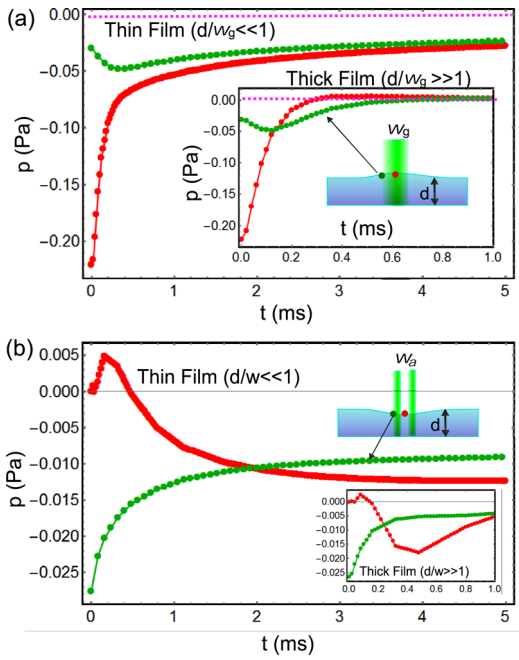

Fig. 4. Numerical simulation, considering (a) thick- and thin-film deformation due to GB and (b) thick- and thin-film deformation due to annular GB. Here $P = 4$ W, $w_g = 250$ μm, and $w_a = 500$ μm.

Here, P_0 and w_g are the power and radius of the Laguerre–Gauss beams LG_{0l}. By putting $l = 0$ and 8 gives the GB and annular GB intensity profiles of the laser beam [31]. The main advantage of FEM calculation is getting the pressure and velocity profile of the deformed surface. This is vital because pressure and velocity finally decide the transient deformation height $h(r, t)$. Figures 4(a) and 4(b) present the pressure and velocity as a function of time which show that in the thin-film case, the pressure to reach equilibrium (across the beam waist) is larger than in the thick-sample case. Initial pressure (at center and beam edge) is also exactly opposite in GB and annular GB cases, which is responsible for the presence of inward pressure.

In conclusion, our experimental setup allowed us to simultaneously observe and distinguish the two rivaling forms of momentum by measuring the nanometric AW interface deformation induced by annular GB excitation. Our experimental results suggested that the observation of momentum at the AW interface depends not only on the incident laser but also on the fluid mechanics. The resultant surface deformation is a complex interplay of fluid dynamics and radiation pressure [19]. Our finding helps in the measurement of light momentum inside a dielectric medium. The result offers significant potential applications in optofluidics [27,28], fluid droplets, and re-configurable lenses.

Funding. Department of Science and Technology of Jilin Province (20200802001GH); National Natural Science Foundation of China (62121005, 62134009).

Acknowledgments. This work was supported by the National Natural Science Foundation of China (grant no. 62121005, 62134009) and Development Program of the Science and Technology of Jilin Province (20200802001GH).

Disclosures. The authors declare no conflicts of interest.

Data availability. Data underlying the results presented in this paper are not publicly available at this time but may be obtained from the authors upon reasonable request.

REFERENCES

1. H. Minkowski, Math. Ann. **68**, 472 (1910).
2. M. Abraham, Rend. Circ. Matem. Palermo **28**, 1 (2009).
3. A. Ashkin and J. M. Dziedzic, Phys. Rev. Lett. **30**, 139 (1973).
4. G. K. Campbell, A. E. Leanhardt, J. Mun, M. Boyd, E. W. Streed, W. Ketterle, and D. E. Pritchard, Phys. Rev. Lett. **94**, 170403 (2005).
5. R. N. C. Pfeifer, T. A. Nieminen, N. R. Heckenberg, and H. Rubinsztein-Dunlop, Rev. Mod. Phys. **79**, 1197 (2007).
6. R. Peierls, Proc. R. Soc. Lond. A **347**, 475 (1976).
7. S. M. Barnett, Phys. Rev. Lett. **104**, 070401 (2010).
8. C. Baxter and R. Loudon, J. Mod. Opt. **57**, 830 (2010).
9. K. J. Webb, Phys. Rev. Lett. **111**, 043602 (2013).
10. U. Leonhardt, Nature **444**, 823 (2006).
11. D. Pile, Nat. Photonics **9**, 418 (2015).
12. N. L. Balazs, Phys. Rev. **91**, 408 (1953).
13. W. Shockley, Phys. Rev. Lett. **20**, 343 (1968).
14. M. Partanen, T. Häyrynen, J. Oksanen, and J. Tulkki, Proc. SPIE **9742**, 974217 (2016).
15. M. Lobet, I. Liberal, L. Vertchenko, A. V. Lavrinenko, N. Engheta, and E. Mazur, Light: Sci. Appl. **11**, 110 (2022).
16. G. Verma and K. P. Singh, Phys. Rev. Lett. **115**, 143902 (2015).
17. G. Verma, K. Chaudhary, and K. P. Singh, Sci. Rep. **7**, 42554 (2017).
18. N. G. C. t. Astrath, Nat. Commun. **5**, 4363 (2014).
19. U. Leonhardt, Phys. Rev. A **90**, 033801 (2014).
20. L. Zhang, W. She, N. Peng, and U. Leonhardt, New J. Phys. **17**, 053035 (2015).
21. O. A. Capeloto, V. S. Zanuto, L. C. Malacarne, M. L. Baesso, G. V. B. Lukasievicz, S. E. Bialkowski, and N. G. C. Astrath, Sci. Rep. **6**, 20515 (2016).
22. J. P. Gordon, Phys. Rev. A **8**, 14 (1973).
23. R. V. Jones and B. Leslie, Proc. R. Soc. Lond. A **360**, 347 (1978).
24. G. Verma, H. Chesneau, H. Chraibi, U. Delabre, R. Wunenburger, and J.-P. Delville, Soft Matter **16**, 7904 (2020).
25. G. Verma and K. P. Singh, Appl. Phys. Lett. **104**, 244106 (2014).
26. G. Verma, G. Yadav, C. S. Saraj, L. Li, N. Miljkovic, J. P. Delville, and W. Li, Light: Sci. Appl. **11**, 115 (2022).
27. C. Psaltis and Demetri. Quake Stephen R. Yang, Nature **442**, 381 (2006).
28. B. J. Monat and C. Domachuk P. Eggleton, Nat. Photonics **1**, 106 (2007).
29. A. Casner and J.-P. Delville, Phys. Rev. Lett. **90**, 144503 (2003).
30. W. Ding, M.R.C. Mahdy, D. Gao, T. Zhang, F. C. Cheong, A. Dogariu, Z. Wang, and C. T. Lim, Light: Sci. Appl. **4**, e278 (2015).
31. G. Verma and G. Yadav, Opt. Lett. **44**, 3594 (2019).